





## Experimental analysis of improved bearing capacity in offshore foundations due to thermal consolidation

Marina de Souza Ferreira<sup>1#</sup> , Fernando Saboya Albuquerque Junior<sup>1</sup> ,  
Sérgio Tibana<sup>1</sup> , Ricardo Garske Borges<sup>2</sup> 

Article

### Keywords

Offshore foundations  
Soft clays  
Soil improvement  
Physical modeling  
Thermal consolidation

### Abstract

The anchoring of floating platforms is one of many processes in the oil industry that requires innovative strategies. In this respect, there is interest in developing techniques that improve the shear strength of soft soils in order to increase the bearing capacity of offshore foundations anchored in these soils. Normally consolidated clay soil is known to undergo thermal consolidation when submitted to temperature cycles. The present study aimed to assess the impact of a temperature cycle on soft kaolin clay using a reduced-scale physical model submitted to heating at maximum temperatures of 85 °C and 65 °C, followed by cooling. Variables such as pore pressure, temperature at different soil depths and displacement were monitored during the thermal cycle to better understand the phenomenon. The strength profile before and after heating was determined via T-bar tests conducted in different positions in relation to the heat source. The temperature variation increased the undrained shear strength of the soil directly proportional to the temperature applied and inversely proportional to the radial distance from the heat source, reaching improvements of 123%. In this respect, it is believed that applying a temperature cycle to normally consolidated soft clayey soil can improve the pullout capacity of offshore foundations.

## 1. Introduction

In terms of fundamental soil mechanical behavior, the relationship between heating and thermal volume changes in clayey soil began to be studied in the 1950s. Finn (1951) conducted laboratory tests to assess the magnitude and rate of consolidation after temperature variations. Later, Campanella & Mitchell (1968) found that when heated, normally consolidated saturated clays initially exhibited increased pore pressure due to the relative difference between the thermal expansion of the soil particles, the solid structure and water. This was followed by thermal consolidation, resulting from the reorganization of contact forces between the soil particles and dissipation of the excess pore pressure caused by the temperature gradient. Since then, researchers have studied the impact of temperature on clayey soils for different purposes.

Baldi et al. (1988) investigated volume changes caused by heating in clays with low porosity and moisture content and observed irreversible shrinking under normally consolidated conditions. Plum & Esrig (1969), Towhata et al. (1993), Cekerevac & Laloui (2004) and Abuel-Naga et al. (2007) also reported shrinkage in normally consolidated clays submitted to heating.

The influence of temperature on the shear strength of clays was demonstrated by Kuntiwattanukul et al. (1995), who heated normally consolidated clays up to 90 °C under drained

conditions and observed an increase in soil stiffness and strength. Trani et al. (2010) heated normally consolidated Bangkok clay up to 90 °C, under drained and undrained conditions, and reported undrained shear strength improvement after one drained heating and cooling cycle. Samarakoon et al. (2018) also found that the undrained shear strength of normally consolidated clays increased when heated under drained conditions, especially after one heating and cooling cycle. Wang & Zhang (2020) assessed thermo-mechanical behavior at the pile-soil interface in soft kaolin clay submitted to temperature variations, using direct shear tests.

As reported by different authors (Houston et al., 1985; Hueckel & Baldi, 1990; De Bruyn & Thimus, 1996; Delage et al., 2000, Cui et al., 2000; Laloui & François, 2009; Di Donna & Laloui, 2015; Coccia & McCartney, 2016; Hong et al., 2016; Zhou & Ng, 2018; Cheng et al., 2020), heating normally consolidated clay increases its shear strength, making this technique particularly appealing in improving the bearing capacity of offshore foundations, where traditional soil improvement methods cannot be applied. Increasing the shear strength of the soil around these foundations enables verticalization of the resulting load and, therefore, fewer mooring lines are needed, which allows for considerable savings at installation of these anchors. Thus, for thermal consolidation to be used as an improvement technique for soft soils, it is important to investigate the influence of a temperature gradient on excess

<sup>#</sup>Corresponding author. E-mail address: marinadesferreira@gmail.com

<sup>1</sup>Universidade Estadual do Norte Fluminense Darcy Ribeiro, Department of Civil Engineering, Campos dos Goytacazes, RJ, Brasil.

<sup>2</sup>CENPES Petrobras Centro de Pesquisa e Desenvolvimento, Rio de Janeiro, RJ, Brasil.

Submitted on November 29, 2021; Final Acceptance on February 4, 2022; Discussion open until May 31, 2022.

<https://doi.org/10.28927/SR.2022.078021>



This is an Open Access article distributed under the terms of the Creative Commons Attribution License, which permits unrestricted use, distribution, and reproduction in any medium, provided the original work is properly cited.

pore pressure, and possible shear strength improvement after its dissipation.

As such, the present study aimed to evaluate a reduced-scale physical model of typical Brazilian marine kaolin clay submitted to maximum temperatures of 65 °C and 85 °C, in order to measure undrained shear strength before and after a heating and cooling cycle with a T-bar penetrometer at different radial distances from the heat source.

## 2. Materials

The reduced-scale physical model was constructed in a 500 mm-long cylindrical container with an internal diameter of 464 mm, which was filled with a mixture of kaolin and metakaolin soil. A torpedo pile was inserted to serve as a heating element, in addition to pore pressure transducers and thermocouples. The experimental apparatus was placed in a hydraulic press (Figure 1), which applies loads via a controlled electric motor to ensure that the load remains constant throughout the test. A CSR-5000 load cell of 50 kN capacity was used.

Because the soil's response to a temperature gradient depends on its degree of pre-consolidation, an apparatus was needed to maintain constant vertical stress throughout the test without having to remove the top cap for the T-bar tests, ensuring that the soil remained normally consolidated. To that end, a special top cap was designed with holes containing self-tapping screws that could be removed after consolidation to allow the T-bar tests to be performed.

A 250 mm-long hollow pile with an external diameter of 25 mm was used as a foundation element and heat source, fitted with a 750 W heating element 180 mm long and 13 mm wide. Implastec thermal paste was inserted into the element to improve heat transfer between the pile and heating element. The thermal load applied by the heater was controlled to ensure that the temperature within the pile remained constant throughout the experiment.

The heating element, which also serves as a pile, was attached to the center of the top cap, with an instrumentation probe positioned on either side, 30 mm from the heat source, each containing sensors to measure the temperature at three different depths and the pore pressure around the heater (Figure 1). The T-bar tests were conducted through the holes in the cap, which were arranged at radial distances of 30 mm, 88 mm and 153 mm ( $r/r_{pile}$  ratio of 2.40, 7.04 and 12.24) from the heat source axis and denominated  $R0$ ,  $R1$  and  $R2$ , respectively.

The experiment was monitored using EPB-PW pore pressure transducers (TE Connectivity), type K thermocouples (Omega TT-K 36-500) and laser displacement sensors (Wenglor CP3MHT80). The locations and nomenclature of the sensors are shown in Figure 2 and Tables 1 and 2, with Table 1 referring to sensors installed on the walls of the container and Table 2 to those on the probe.

In addition to the sensors presented, four thermocouples were installed, two directly above the top cap to measure room temperature ( $TC1$  and  $TC2$  AMB) and two below it to

measure the temperature on the soil surface. Three additional thermocouples were positioned on the surface of the torpedo pile to supply the temperature control system.

T-bar penetrometer tests were performed to obtain the undrained soil shear strength profile. The length and diameter of the penetrometer were 14 and 7 mm, respectively, and undrained shear strength ( $S_u$ ) was calculated as proposed by Stewart & Randolph (1991):

$$S_u = \frac{F_v}{N_b DL} \quad (1)$$

where  $F_v$  is the vertical force during penetration, measured by the strain gauge coupled to the T-bar,  $N_b$  is the T-bar factor, and  $D$  and  $L$  are its diameter and length, respectively.

The soil used in the experiment was a mixture of 40% kaolin and 60% metakaolin (dry weight) and its properties are presented in Table 3.

**Table 1.** Depth, from the upper surface of the container, and nomenclature of each sensor on the container walls.

	Depth (mm)	Nomenclature
Side 1	200	PP C11
	270	PP C12
	340	PP C13
Side 2	200	PP C21
	270	PP C22
	340	PP C23

**Table 2.** Depth, from the lower surface of the top cap, and nomenclature of the sensors on the probes.

Pore pressure transducer probes		
	Depth (mm)	Nomenclature
Side 1	125	PP S1
Side 2	125	PP S2
Thermocouple probes		
	Depth (mm)	Nomenclature
Side 1	50	TC S11
	80	TC S12
	110	TC S13
Side 2	50	TC S21
	80	TC S22
	110	TC S23

**Table 3.** Physical characterization of the kaolin and metakaolin mixture.

Parameter	Value
Liquid limit (%)	45.4
Plastic limit (%)	26.5
Plasticity index (%)	18.9
Specific gravity	2.64
Hygroscopic moisture content (%)	0.64
Colloidal Activity	0.53

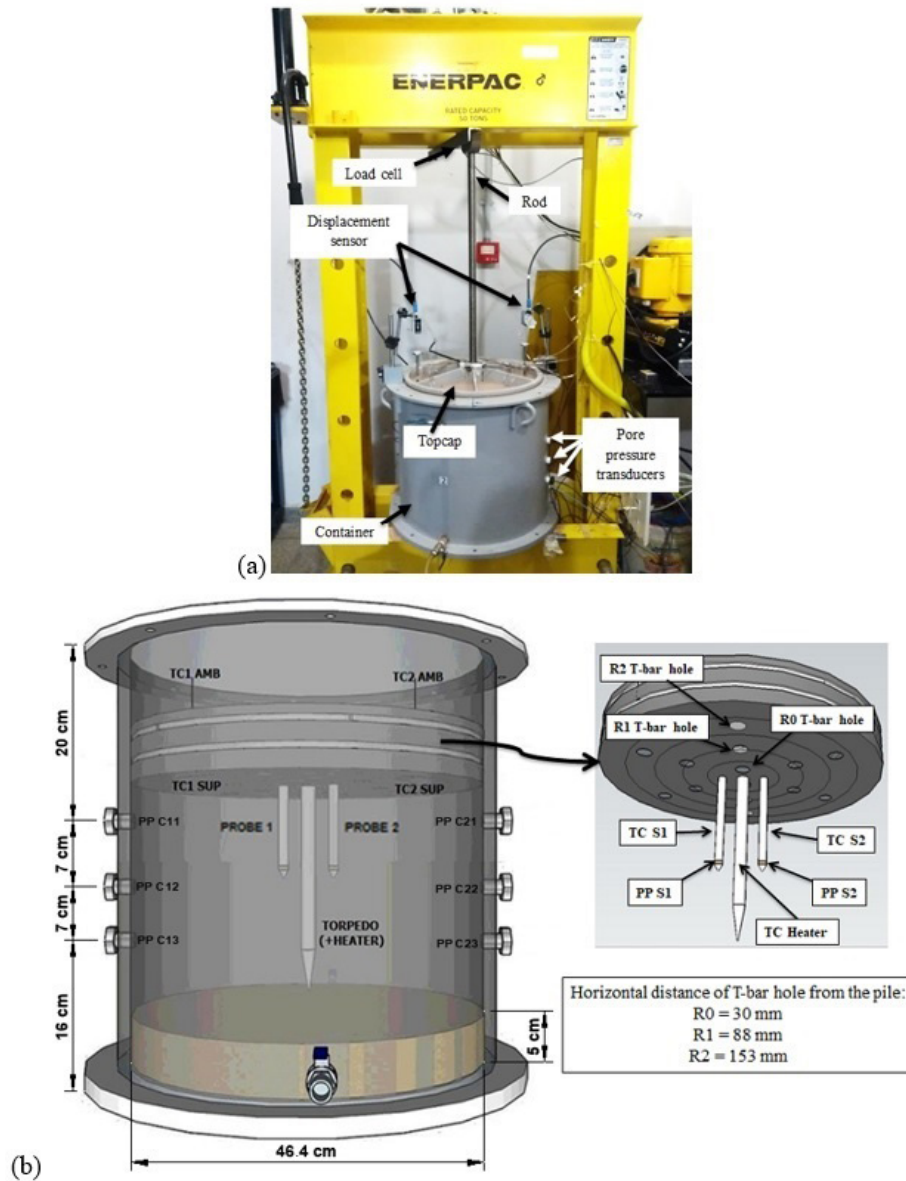


Figure 1. (a) Equipment used to construct the model for testing; (b) Insert of the instruments used in the container and top cap.

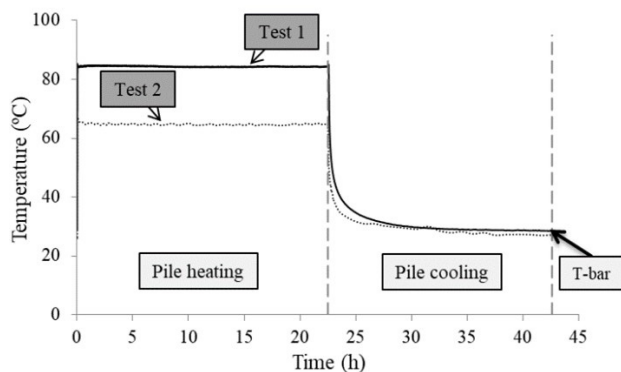


Figure 2. Scheme of stages in tests 1 and 2.

### 3. Methodology

Two tests were conducted for the present study, each at a different maximum temperature (85 °C and 65 °C), in order to assess the change in soil shear strength after a temperature cycle. The general methodology applied in each test was identical, the heating temperature being the only difference, as presented in Table 4.

#### 3.1 Slurry preparation, mechanical consolidation, and reference T-bar

For slurry preparation, powdered soil was mixed with distilled deaerated water to obtain an approximate moisture

content of 68.1%, followed by homogenization for 30 minutes in a mechanical mixer. Next, the mixture was placed in a vacuum deaerator for 30 minutes to ensure complete saturation and minimize air bubbles.

During mechanical consolidation, loading was performed in stages, applying approximately double the previous load in each stage, with final vertical stress of 50 kPa. The subsequent loads were applied in magnitudes of 5 kPa, 12.5 kPa, 25 kPa and 50 kPa, only once the system had stabilized from the previous stage. Table 5 shows the void ratio ( $e_p$ ) and moisture ( $w_p$ ) content after mechanical consolidation, void ratio ( $e_0$ ) and moisture content ( $w_0$ ) of the slurry before mechanical consolidation, and the compression index ( $C_c$ ) in both tests.

These tests made it possible to obtain  $t_{90}$  and estimate the coefficient of consolidation ( $c_v$ ) via Taylor’s method (1942) for loads of 12.5 kPa, 25 kPa and 50 kPa, as summarized in Table 6. By determining  $c_v$ , the normalized penetration rate of the T-bar penetrometer can be calculated.

At the end of mechanical consolidation, the screws in positions  $R1$  and  $R2$  on the top cap were removed in order to perform the T-bar test and obtain the undrained shear strength profile of the soil before thermal consolidation, denominated the reference profile. The penetration rate was 16 mm/s, calculated as a function of the  $c_v$  of the material, as proposed by Finnie & Randolph (1994).

### 3.2 Temperature cycle and final T-bar

Heating of the pile began once the undrained shear strength profile (reference) of the soil had been obtained. As previously mentioned, the target temperatures for tests 1 and 2 were 85 °C and 65 °C, respectively. In each test, under constant vertical stress of 50 kPa, the system was allowed to stabilize through dissipation of the excess pore pressure caused by heating. This stage lasted around 22 hours for both tests.

**Table 4.** Summary of the test stages.

Testing stage	Stage Description
i	Slurry preparation
ii	Consolidation
iii	Reference T-bar
iv	Pile heating
v	Pile cooling
vi	T-bar after temperature cycle

**Table 5.** Soil moisture content and void ratio before and after mechanical consolidation and compression index for both tests.

Test	$e_0$	$w_0$ (%)	$e_f$	$w_f$ (%)	$C_c$
1	1.77	68.91	1.24	32.88	0.21
2	1.76	68.72	1.23	32.71	0.17

Following the heating stage, the heater was switched off and the sensors allowed to stabilize by lowering the temperature and pore pressure to the initial values, which took approximately 22 hours. Next, the T-bar tests were conducted at radial distances  $R0$ ,  $R1$  and  $R2$  for each test, in order to establish a panorama of the change in undrained shear strength with temperature and distance from the heat source. Figure 2 presents the scheme of the stages covered in this item.

## 4. Results and discussion

### 4.1 Reference T-bar

Two T-bars were used for each test to obtain the reference strength. For the subsequent strength improvement analyses, the mean between the two reference T-bars for each individual test was used along the entire depth of the model. Thus, given the homogeneity of the soil prepared, the soil in the model was deemed to exhibit this same initial undrained shear strength profile. It is important to underscore that the first 50 mm of soil were disregarded in the analyses because disturbances were observed in this zone, resulting from interaction between the soil surface and the top cap of the container.

The average undrained shear strength profile for each test is shown in Figure 3a. For both tests, strength was greater in the upper section of the model, due to the uneven distribution of the vertical load impacted by possible lateral friction between the wall of the container and the top cap. Additionally, the absolute strength values across the soil depth were used to calculate relative frequency distribution for both tests, as shown in Figure 3b. It should be noted that the mean undrained shear strength was 11.6 kPa and 14.0 kPa for tests 1 and 2, respectively.

### 4.2 Temperatures

The normalized temperature during heating was calculated based on the fact that the maximum temperatures of 85 °C and 65 °C in tests 1 and 2, respectively, generated approximate respective increases of 55 °C and 39 °C in the pile. To that end, the increase of temperature recorded by each sensor was normalized by the temperature increase of the heating element ( $dT_{Heater}$ ). The increase of temperature of all the sensors



were calculated by subtracting the temperature registered by the respective sensor ( $TC$ ) from the room temperature ( $TC_{AMB}$ ) at the beginning of the test. The curves of temperature increase normalized by the rise in heater temperature for the sensors at different depths, on the soil surface and in the room, are presented in Figure 4.

Regarding normalized temperature increases, the largest increases for the probe sensors located at a radial distance of 3 cm from the pile axis were measured in the sensor closest to the center of the heater, at a depth of 11 cm. The sensors closest to the heater recorded a 40% temperature increase in test 1 and 35% in test 2 in relation to the temperature increase of the pile, whereas the maximum temperature rise in those furthest from the heater, installed on the soil surface, was 21% in test 1 and 10% in test 2. Increases in the remaining sensors were inversely proportional to distance from the heater. There was also a slight increase in the room temperature during the heating stage.

Once the established maximum temperature had been reached, the heating system was switched off and the sensors were allowed to cool naturally until the end of the cooling stage, approximately 20 hours after shutoff.

### 4.3 Soil response

Undrained heating caused an instantaneous increase in pore pressure in the sensors installed on the probes, which subsequently dissipated after 7 hours (Figure 5) of heating; values are summarized in Table 7. As expected, the increase in pore pressure was greater at higher temperatures.

With respect to deformation, no significant changes in settlement were observed in the displacement sensors in either the heating or cooling stages. However, localized deformation is believed to have occurred in the area around

**Table 6.** Coefficient of consolidation ( $c_v$ ) and  $t_{90}$  during mechanical consolidation conducted in stages.

Assumed vertical effective stress (kPa)	$t_{90}$ (h)	$c_v$ (cm <sup>2</sup> /s)
12.5	12.7	6.7E-03
25.0	11.3	7.2E-03
50.0	6.5	1.2E-02

**Table 7.** Peak pore pressure due to heating in tests 1 and 2.

Test	Sensor	Maximum pore pressure increase (kPa)	Mean pore pressure increase (kPa)
1	S1	7.77	7.36
	S2	6.94	
2	S1	4.08	4.16
	S2	4.23	

the heat source, due to the dissipation of excess pore pressure measured during soil heating.

### 4.4 Undrained shear strength improvement

After application of the temperature cycle, the soil strength profile for the different radial distances from the heat source was obtained via T-bar tests. Strength improvement due to thermal consolidation, expressed in percentage, was calculated by subtracting the mean reference strength from the strength obtained after the temperature cycle ( $dS_u$ ) and dividing the result by the mean reference strength ( $S_{u,ref}$ ) along the entire depth of the model. This made it possible to obtain a net undrained shear strength improvement profile for each radial distance in each test.

The strength profiles obtained across the soil depth were used to determine the relative frequency distributions of these gains for the different temperatures and radial distances. The histograms showed improvements of 20% to 270% at intervals of 50%.

It should be noted that the strength improvement analyses were interested in two different ways, considering

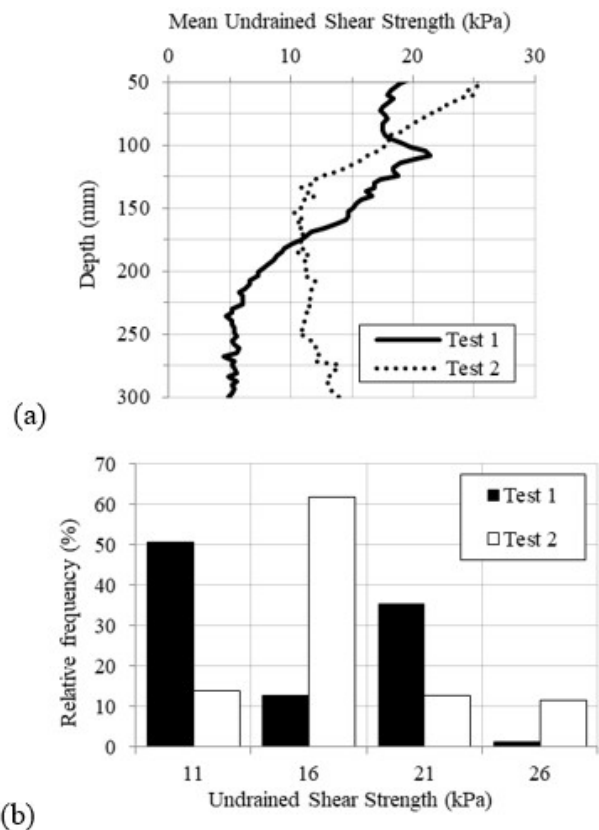


**Figure 3.** (a) Mean reference undrained shear strength profile for tests 1 and 2; (b) Distribution of relative frequencies for mean reference undrained shear strength along the length of the model, for tests 1 and 2.

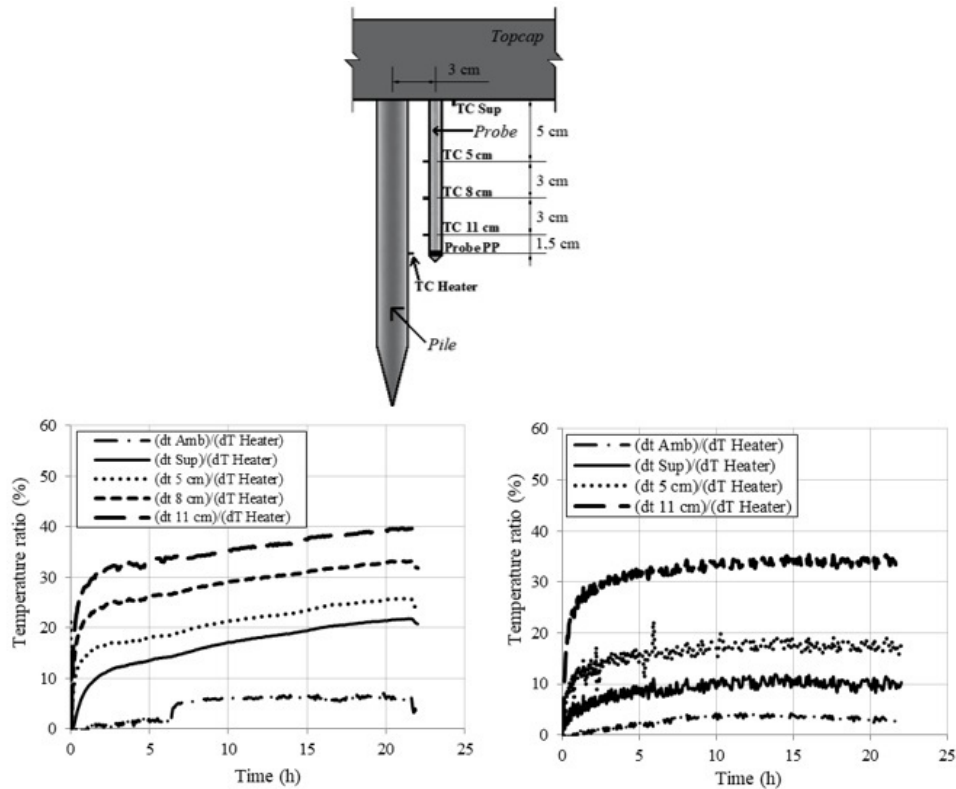


Figure 4. Distribution of temperatures normalized (dt) with time during heating, in tests 1 and 2, respectively.

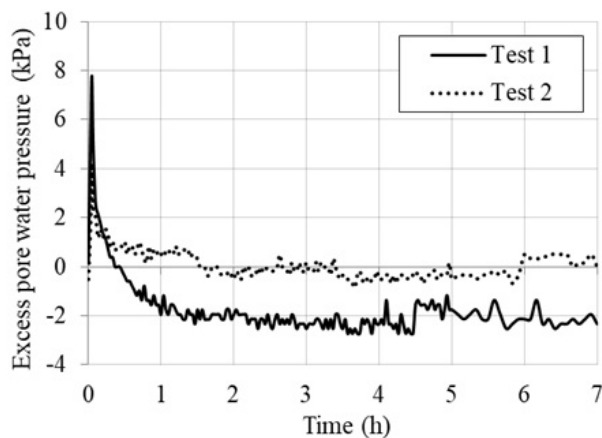


Figure 5. Pore pressure in the probes during the heating stage for tests 1 and 2.

the maximum temperature applied to the soil and in terms of the radial distance of the T-bar from the heat source.

#### 4.4.1 Analysis of shear strength improvement by radial distance

The shear strength improvement profile and its distribution frequency are presented in Figure 6 for radial distances of

30 mm, 88 mm and 153 mm from the heat source in test 1. Mean undrained shear strength was 24.2 kPa, 15.3 kPa and 12.4 kPa for distances  $R_0$ ,  $R_1$  and  $R_2$ , respectively, in test 1, which generated net strength improvements of 123%, 58% and 14% for the respective radial distances. These results indicate that improvement was directly proportional to proximity to the heat source. Additionally, the greatest strength improvements were observed close to a depth of 200 mm for distances  $R_0$  and  $R_1$ . On the other hand, the T-bar test performed at  $R_2$  exhibited a more homogeneous improvement profile with depth and less improvement in relation to distances closer to the heat source.

In test 2, the mean undrained shear strength values were 22.8 kPa, 18.9 kPa and 16.6 kPa for  $R_0$ ,  $R_1$  and  $R_2$ , respectively, generating net undrained shear strength improvements of 74%, 36% and 19% with the temperature cycle.

The proportionality between shear strength improvement and proximity to the heat source can once again be observed in the histograms in Figure 7. There is clearly a greater concentration of larger improvements for T-bars closer to the heat-producing pile.

#### 4.4.2 Analysis of improvement according to temperature

Shear strength improvement according to temperature was analyzed by considering each individual radial distance

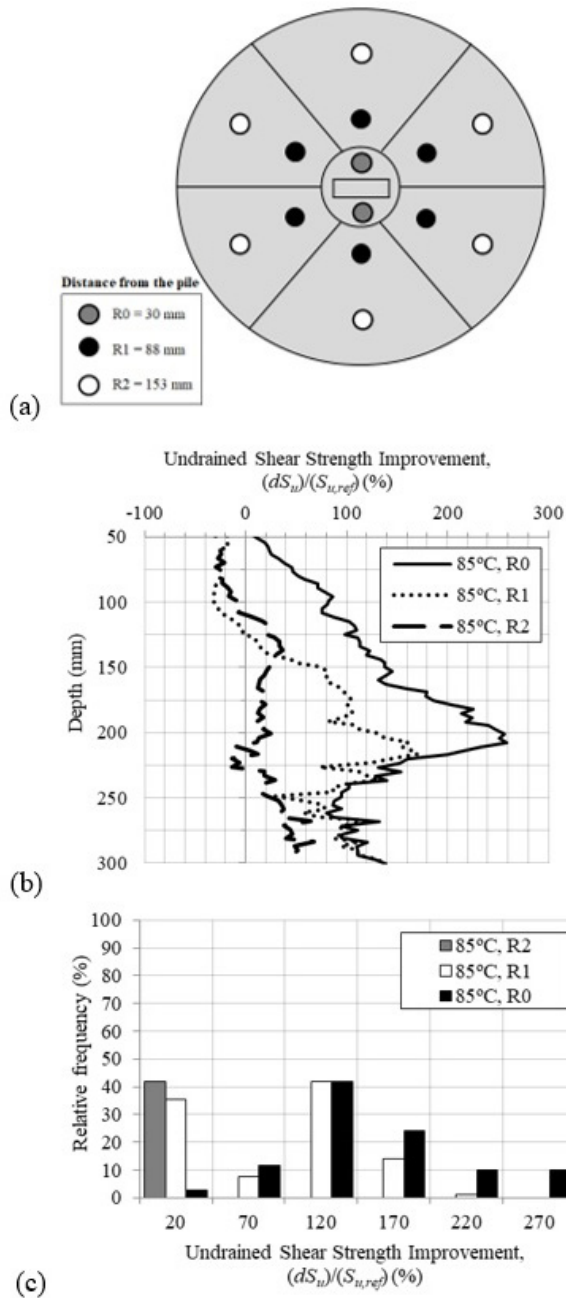


**Figure 6.** (a) Location of top cap holes in top view; (b) Shear strength improvement profiles at different radial distances for test 1; (c) Distribution of relative frequencies for undrained shear strength improvement at different radial distances for test 1.

and varying the maximum temperatures applied to the soil. The strength improvement calculation was performed by subtracting the strength obtained after the thermal cycle from the reference strength and dividing this value by the reference strength. In addition, the improvement was given in percentage.

For the T-bar closest to the heat source, *R0*, both tests clearly show that increases in strength were directly proportional to the level of heating applied, with average improvements of

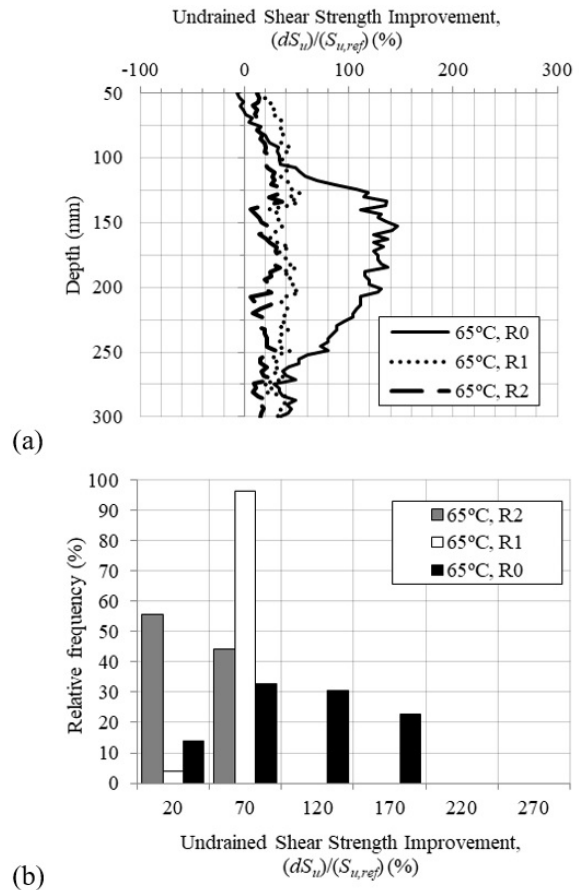


**Figure 7.** (a) Shear strength improvement profiles at different radial distances for test 2; (b) Distribution of relative frequencies for undrained shear strength improvement at different radial distances for test 2.

123% and 74% for soil heated at 85 °C and 65 °C, respectively (Figure 8). The histograms in Figure 8 reinforce observations of the shear strength improvement profiles, where there is a larger concentration of improvements at higher values for soil heated at the highest temperature.

The shear strength improvement profiles for distance *R1*, 88 mm from the pile axis, are shown in Figure 9 for the different temperatures tested. Once again, greater improvements occurred in soil heated at 85 °C, that is, at this radial distance, increased shear strength is directly proportional to the level of heat applied to the clay.

Figure 10 presents the shear strength improvement profiles and relative histograms at distance *R2* for the different tests. Based on the different improvement profiles in the Figure 9, the heating level was not relevant for the increase in shear strength at this radial distance.

#### 4.5 Estimating pile pullout capacity

The average values of changes in undrained shear strength made it possible to estimate the pullout capacity of

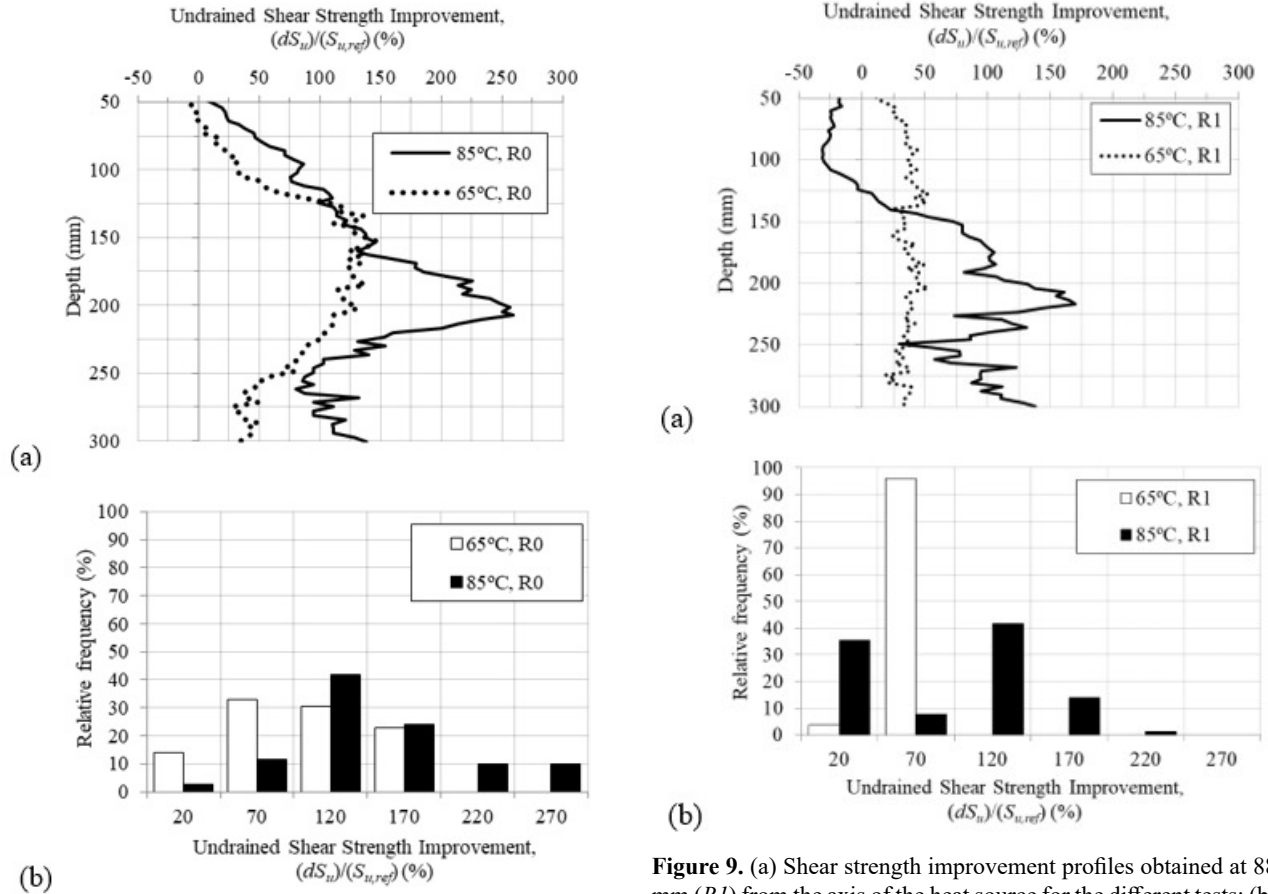


**Figure 8.** (a) Shear strength improvement profiles obtained at 30 mm (*R0*) from the axis of the heat source for the different tests; (b) Distribution of relative frequencies for undrained shear strength improvement at a radial distance of 30 mm (*R0*) in the different tests.

the pile. To that end, the mean shear strength variation was related to the normalized distance from the heat source for each test, as shown in Figure 11, which exhibits a nonlinear relationship between distance and shear strength variation.

Based on the relationship depicted in Figure 11, shear strength variation at the pile-soil interface and pile pullout capacity before and after the temperature cycle can be estimated, in order to assess the impact of the temperature gradient. To that end, the normalized distance for the pile-soil interface was analyzed and  $S_u/S_{u,ref}$  values of 2.63 and 2.00 were found for tests 1 and 2, respectively. Thus, mean undrained shear strength values of 30.6 kPa and 28.1 kPa were recorded at the pile-soil interface for tests 1 and 2, respectively.

Based on shear strength at the interface, the pullout capacity of the pile was estimated using the Alpha method, described by Bai & Bai (2014), with the equation:

$$Q = \alpha S_u A \quad (2)$$

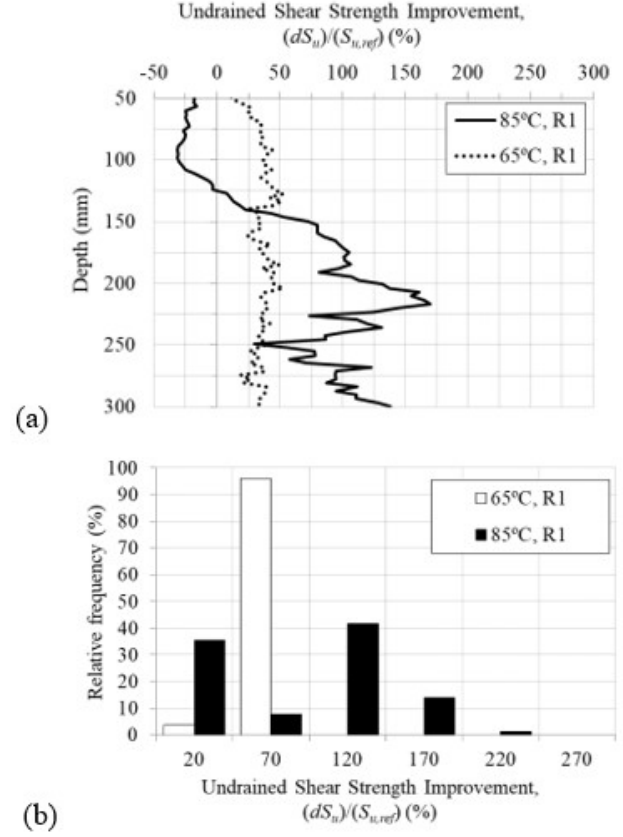


**Figure 9.** (a) Shear strength improvement profiles obtained at 88 mm (*R1*) from the axis of the heat source for the different tests; (b) Distribution of relative frequencies for undrained shear strength improvement at a radial distance of 88 mm (*R1*) in the different tests.

where  $Q$  is pullout capacity,  $\alpha$  the cohesion factor,  $S_u$  undrained shear strength of the soil and  $A$ , the lateral area of the pile. According to the author, the cohesion factor can be calculated as follows:

$$\alpha = 0.608 - 0.123S_u - \frac{0.274}{S_u^2 + 1} + \frac{0.695}{S_u^3 + 1} \quad (3)$$

with undrained shear strength ( $S_u$ ) expressed in ksf. In the case of the model, the diameter (13 mm) and length (250 mm) of the pile correspond to an area of 102.1 cm<sup>2</sup> or 0.0102 m<sup>2</sup>. The calculations for  $\alpha$  cohesion factor of pile pullout capacity and net improvement ( $\Delta Q$ ) are presented in Table 8, for strength values before and after thermal treatment.

As demonstrated, there were relevant increases in pile pullout capacity due to the temperature cycle, with net improvement of 132% and 83% in tests 1 and 2, respectively.

The net improvement in pullout capacity was also plotted as a function of the temperature increase experienced by the pile, as shown in Figure 12. The figure also presents data on the reduced-scale physical model tested by Ghaawd (2018),



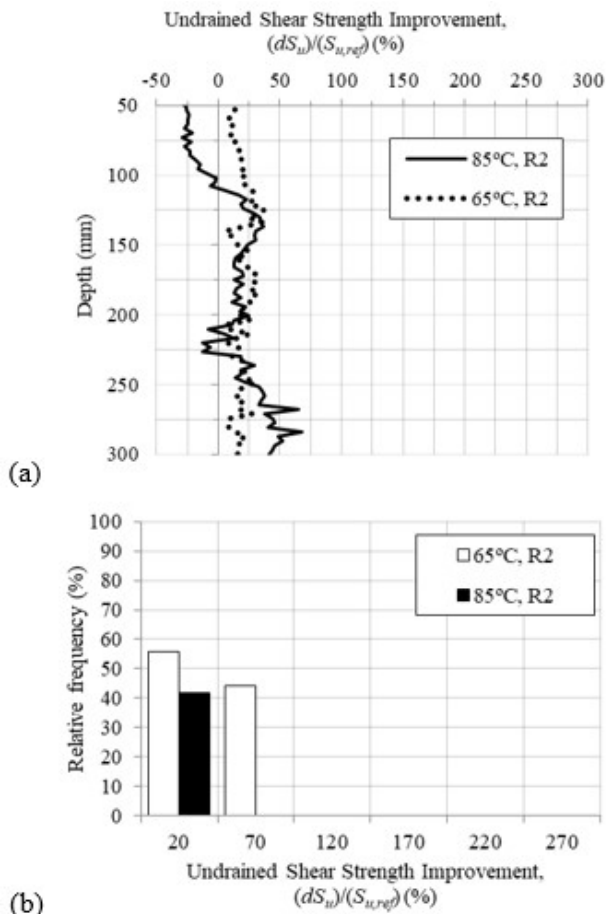


**Figure 10.** (a) Shear strength improvement profiles obtained 153 mm ( $R_2$ ) from the axis of the heat source for the different tests; (b) Distribution of relative frequencies for undrained shear strength improvement at a radial distance of 153 mm ( $R_2$ ) in the different tests.

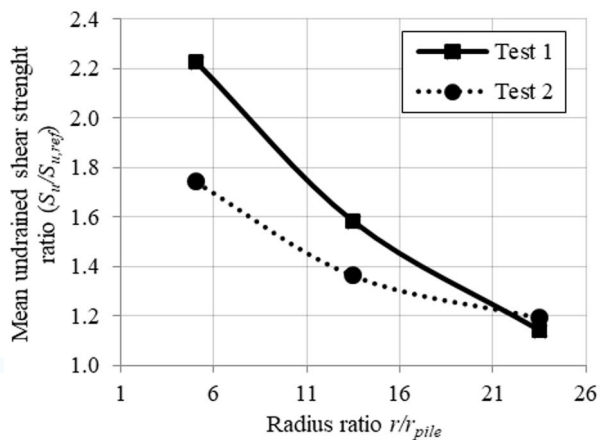


**Figure 11.** Undrained shear strength after the temperature cycle normalized by the reference shear strength versus distance normalized by the radius of the pile for tests 1 and 2.

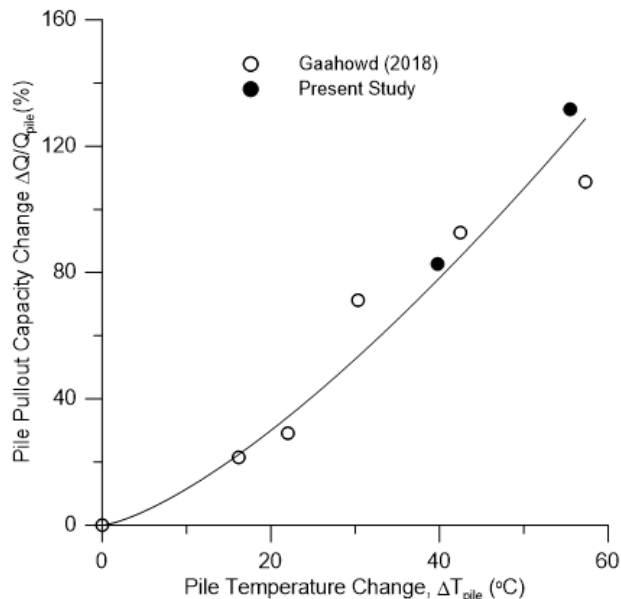


**Figure 12.** Pile Pullout Capacity Change with induced temperature after thermal consolidation.

**Table 8.** Estimated pullout capacity of the piles before and after the temperature cycle for tests 1 and 2.

T-bar	$S_u$ (kPa)	$\alpha$	$Q$ (N)	$\Delta Q$ (%)
Reference, Test 1	11.63	1.00	119.33	131.89
Test 1	30.58	0.89	276.71	
Reference, Test 2	14.04	1.00	142.98	82.54
Test 2	28.08	0.91	261.00	

where a miniature torpedo pile was subjected to different temperature cycles in a 50g gravitational field. There is good agreement between the curve obtained from the data in the present study and the data reported by the aforementioned author. It is important to mention that, despite both studies were carried out in different gravity fields, the direct comparison is possible to be made because the variables are expressed in non-dimensional way, which is, in turn, should not be dependent on the scale.

### 5 Conclusions

Given the need to develop techniques to improve the bearing capacity of offshore foundations in soft clayey soils, the present study aimed to better understand the impact of a temperature cycle on the thermal and mechanical behavior of a soft kaolin clay, using a reduced-scale physical model with a miniature torpedo pile as a heat source, inserted into the soil in question.

Two tests were conducted with reduced-scale models, where soil under constant vertical stress of 50 kPa was submitted to increasing temperatures, reaching maximums of 85 °C and 65 °C, and then cooled. The heating cycle caused consolidation, improving the undrained shear strength of the soil in direct proportion to the temperature level applied and inversely proportional to the radial distance from the heat source. In the T-bar tests closest the pile, at 30 mm, the mean net improvements in undrained shear strength were 123% and 74% for tests 1 and 2, respectively.

Additionally, the pullout capacity of the pile before and after the temperature cycle was estimated, thereby generating net pullout capacity increases of 132% and 83% for tests where the soil was heated at 85 °C and 65 °C, respectively.

As such, we believe that this procedure has considerable potential as an improvement technique for soft soils, in order to increase the bearing capacity of offshore foundations.

## Acknowledgements

The Authors are grateful to Petrobras for the financial support of this research (Grant NO SAP: 4600499688, Jur: 0050.0098204.15.9). The first Author is also grateful to the Brazilian Scholarship Agency – CAPES for financing the scholarship during the development of her PhD Thesis).

## Declaration of interest

The authors have no conflicts of interest to declare. All co-authors have observed and affirmed the contents of the paper and there is no financial interest to report.

## Authors' contributions

Marina de Souza Ferreira: conceptualization, Data curation, Formal analysis, Investigation, Methodology, Validation, Visualization, Writing – original draft, Writing – review & editing. Fernando Saboya Albuquerque Junior: conceptualization, Formal analysis, Methodology, Project administration, Supervision, Writing – review & editing. Sérgio Tibana: conceptualization, Formal analysis, Methodology, Project administration, Supervision. Ricardo Garske Borges: conceptualization, Resources, Funding acquisition, Supervision.

## List of symbols

$A$	Lateral area of the pile
$C_c$	Compression index
$c_v$	Coefficient of consolidation
$D$	T-bar diameter
$dS_u$	Reference mean strength subtracted from strength after thermal cycle
$dT$	Temperature variation
$e_0$	Void ratio of the slurry before mechanical consolidation

$e_f$	Void ratio of the soil after mechanical consolidation
$F_v$	Vertical force during T-bar penetration
$L$	T-bar length
$N_b$	T-bar factor
$PP$	Pore pressure transducer
$Q$	Pullout capacity
$r$	Radial distance from the center of the pile
$R0$	Nomenclature used to the distance of 30 mm from the center of the pile
$r_{pile}$	Pile radius
$R1$	Nomenclature used to the distance of 88 mm from the center of the pile
$R2$	Nomenclature used to the distance of 153 mm from the center of the pile
$S_u$	Undrained shear strength of the soil
$S_{u,ref}$	Reference undrained shear strength of the soil
$SI$	Side 1 sensor
$S2$	Side 2 sensor
$t_{90}$	Time to 90% of consolidation
$TC$	Thermocouple
$w_0$	Moisture content of the slurry before mechanical consolidation
$w_f$	Moisture content of the soil after mechanical consolidation
$\alpha$	Cohesion factor
$\Delta Q$	Net improvement of pile pullout capacity

## References

- Abuel-Naga, H.M., Bergado, D.T., & Bouazza, A. (2007). Thermally induced volume change and excess pore water pressure of soft Bangkok clay. *Engineering Geology*, 89(1-2), 144-154. <http://dx.doi.org/10.1016/j.enggeo.2006.10.002>.
- Bai, Q., & Bai, Y. (2014). *Subsea pipeline design, analysis, and installation*. Waltham: Gulf Professional Publishing.
- Baldi, G., Hueckel, T., & Pellegrini, R. (1988). Thermal volume changes of the mineral-water system in low-porosity clay soils. *Canadian Geotechnical Journal*, 25(4), 807-825. <http://dx.doi.org/10.1139/t88-089>.
- Campanella, R.G., & Mitchell, J.K. (1968). Influence of temperature variations on soil behavior. *Journal of the Soil Mechanics and Foundations Division*, 94(3), 709-734. <http://dx.doi.org/10.1061/JSFEAQ.0001136>.
- Cekerevac, C., & Laloui, L. (2004). Experimental study of thermal effects on the mechanical behavior of a clay. *International Journal for Numerical and Analytical Methods in Geomechanics*, 28(3), 209-228. <http://dx.doi.org/10.1002/nag.332>.
- Cheng, W., Hong, P.Y., Pereira, J.M., Cui, Y.J., Tang, A.M., & Chen, R.P. (2020). Thermo-elasto-plastic modeling of saturated clays under undrained conditions. *Computers and Geotechnics*, 125, 103688. <http://dx.doi.org/10.1016/j.compgeo.2020.103688>.

- Coccia, C.J.R., & McCartney, J.S. (2016). Thermal volume change of poorly draining soils II: model development and experimental validation. *Computers and Geotechnics*, 80(SM3), 16-25. <http://dx.doi.org/10.1016/j.compgeo.2016.06.010>.
- Cui, Y.J., Sultan, N., & Delage, P. (2000). A thermomechanical model for saturated clays. *Canadian Geotechnical Journal*, 37(3), 607-620. <http://dx.doi.org/10.1139/t99-111>.
- De Bruyn, D., & Thimus, J.F. (1996). The influence of temperature on mechanical characteristics of Boom clay: the results of an initial laboratory programme. *Engineering Geology*, 41(1-4), 117-126. [http://dx.doi.org/10.1016/0013-7952\(95\)00029-1](http://dx.doi.org/10.1016/0013-7952(95)00029-1).
- Delage, P., Sultan, N., & Cui, Y.J. (2000). On the thermal consolidation of Boom clay. *Canadian Geotechnical Journal*, 37(2), 343-354. <http://dx.doi.org/10.1139/t99-105>.
- Di Donna, A., & Laloui, L. (2015). Response of soil subjected to thermal cyclic loading: experimental and constitutive study. *Engineering Geology*, 190, 65-76. <http://dx.doi.org/10.1016/j.enggeo.2015.03.003>.
- Finn, F. (1951). The effect of temperature on the consolidation characteristics of remolded clay. *ASTM Special Technical Publication*, 126, 65-71. <http://dx.doi.org/10.1520/STP48297S>.
- Finnie, I. M. S., & Randolph, M. (1994). Punch-through and liquefaction induced failure of shallow foundations on calcareous sediments. In *Seventh International Conference on the Behaviour of Offshore Structures* (vol. 1, pp. 217-230), Massachusetts.
- Ghaaowd, I. (2018). *Thermal improvement of the pullout capacity of offshore piles in soft clays* [Doctoral thesis, University of California San Diego]. University of California at San Diego's repository. Retrieved in November 29, 2021, from <https://escholarship.org/uc/item/30z9k89d>
- Hong, P.Y., Pereira, J.M., Cui, Y.J., & Tang, A.M. (2016). A two-surface thermo-mechanical model for saturated clays. *International Journal for Numerical and Analytical Methods in Geomechanics*, 40(7), 1059-1080. <http://dx.doi.org/10.1002/nag.2474>.
- Houston, S.L., Houston, W.N., & Williams, N.D. (1985). Thermo-mechanical behavior of seafloor sediments. *Journal of Geotechnical Engineering*, 111(11), 1249-1263. [http://dx.doi.org/10.1061/\(ASCE\)0733-9410\(1985\)111:11\(1249\)](http://dx.doi.org/10.1061/(ASCE)0733-9410(1985)111:11(1249)).
- Hueckel, T., & Baldi, G. (1990). Thermoplasticity of saturated clays: experimental constitutive study. *Journal of Geotechnical Engineering*, 116(12), 1778-1796. [http://dx.doi.org/10.1061/\(ASCE\)0733-9410\(1990\)116:12\(1778\)](http://dx.doi.org/10.1061/(ASCE)0733-9410(1990)116:12(1778)).
- Kuntiwattanakul, P., Towhata, I., Ohishi, K., & Seko, I. (1995). Temperature effects on undrained shear characteristics of clay. *Soil and Foundation*, 35(1), 147-162. <http://dx.doi.org/10.3208/sandf1972.35.147>.
- Laloui, L., & François, B. (2009). ACMEG-T: soil thermoplasticity model. *Journal of Engineering Mechanics*, 135(9), 932-944. [http://dx.doi.org/10.1061/\(ASCE\)EM.1943-7889.0000011](http://dx.doi.org/10.1061/(ASCE)EM.1943-7889.0000011).
- Plum, R.L., & Esrig, M.I. (1969). Some temperature effects on soil compressibility and pore water pressure. *Highway Research Board*, 103, 231-242.
- Samarakoon, R., Ghaaowd, I., & McCartney, J.S. (2018). Impact of drained heating and cooling on undrained shear strength of normally consolidated clay. In *Energy Geotechnics. SEG 2018* (pp. 243-249). Cham: Springer. [https://doi.org/10.1007/978-3-319-99670-7\\_31](https://doi.org/10.1007/978-3-319-99670-7_31).
- Stewart, D. P., & Randolph, M. F. (1991). A new site investigation tool for the centrifuge. In *Proceedings of the International Conference on Centrifuge Modelling* (91, pp. 531-538), Boulder.
- Towhata, I., Kuntiwattanaku, P., Seko, I., & Ohishi, K. (1993). Volume change of clays induced by heating as observed in consolidation tests. *Soil and Foundation*, 33(4), 170-183. [http://dx.doi.org/10.3208/sandf1972.33.4\\_170](http://dx.doi.org/10.3208/sandf1972.33.4_170).
- Trani, L.D.O., Bergado, D.T., & Abuel-Naga, H. (2010). Thermomechanical behavior of normally consolidated soft Bangkok clay. *International Journal of Geotechnical Engineering*, 4(1), 31-44. <http://dx.doi.org/10.3328/IJGE.2010.04.01.31-44>.
- Wang, J., & Zhang, Z. (2020). Experimental studies on thermo-mechanical coupled behavior of pile-clay interface. *IOP Conference Series Earth and Environmental Science*, 455(1), 012113. <http://dx.doi.org/10.1088/1755-1315/455/1/012113>.
- Zhou, C., & Ng, C.W.W. (2018). A new thermo-mechanical model for structured soil. *Geotechnique*, 68(12), 1109-1115. <http://dx.doi.org/10.1680/jgeot.17.T.031>.